

# Workspace Investigation of a 3 DOF Compliant Micro-motion Stage

Daniel C. Handley, Tien-Fu Lu<sup>\*</sup>, Yuen Kuan Yong, Craig Eales  
School of Mechanical Engineering, The University of Adelaide

## ABSTRACT

This paper investigates the workspace of a three degree-of-freedom (DOF) compliant micro-motion stage with flexure hinges. This micro-motion stage has parallel structure for better stiffness and accuracy than serial structures and is driven by three PZT stack actuators. This kind of micro-motion stage can be used in applications including micro system assembly, biological cell manipulation and microsurgery. Nevertheless, workspace is fundamental. When selecting or designing micro-motion stage(s) for a particular application, its workspace must be studied to ensure the end-effector can reach the desired points with required orientations. In this paper the workspace of the presented micro-motion stage is investigated and presented, both mathematically and empirically.

## 1. INTRODUCTION

Due to the vast possible applications in areas such as micro-manufacturing, micro-system assembly, biological cell manipulation in biotechnology and MEMs, the demand of ultra-precision manipulation positioning systems is ever increasing. This demand mainly comes from the need to manipulate micro scale objects and perform very small motions, say less than 100  $\mu\text{m}$ . To address this demand, various micro-motion systems have been developed including the use of conventional technologies that can be found in numerous commercially available products.

With inherent problems, such as clearance, friction and backlash, conventional technologies based on servomotors, ball screws, and rigid linkages struggle to fulfill the growing need of even finer motions, such as motions of nanometre scale, with ultra-high positioning accuracy. By contrast, compliant mechanisms, which move solely through the deformation of flexures, provide smooth motion with no backlash, wear or Coulomb friction. As there are no hard non-linearities in the compliant mechanism behavior, there are no physical limitations on the resolution of position control. Therefore, a compliant micro-motion mechanism is able to provide ultra-high precision positioning. Furthermore, parallel structures have higher mechanical stiffness, faster manipulation and higher positioning accuracy<sup>5</sup>, and all the actuators can be located at the base, thus reducing the active mobile mass<sup>6</sup> and leading to higher loading capacity. Due to

these advantages, compliant mechanisms with parallel structures and novel actuators, such as piezoelectric actuators, have been adopted in many designs of micro-motion devices<sup>1-7</sup>.

Despite all the advantages aforementioned, there are some disadvantages associated with compliant micro-motion stages with parallel structures and flexure hinges. For example, the workspace is limited by not only the link lengths and topology of the mechanism but also the material strength and geometry of the hinges. In addition, it is more difficult and complicated to accurately model, analyse, and control compliant mechanisms than conventional mechanisms. This can be partly attributed to hinge compliance in the undesired directions that cause unintended motions that are not mathematically modeled. Coupling between actuator inputs is another common problem that results in complex controller design and modeling for this kind of micro-motion system, unless a particular uncoupled design can be obtained<sup>7</sup>.

This paper presents the workspace investigation of a particular three DOF compliant micro-motion stage with flexure hinges. Firstly, the design of this particular 3 DOF compliant micro-motion stage is presented. Then, the pseudo-rigid-body model (PRBM) is formulated and the theoretical forward kinematics in the form of a constant Jacobian matrix is derived<sup>8</sup>. For comparison purpose, an experimentally determined constant Jacobian matrix is presented next, together with the descriptions of the experiments and experimental set-up. Applying the obtained theoretical Jacobian matrix and experimental Jacobian matrix, the theoretical workspace and experimental workspace of the presented particular compliant micro-motion stage are then plotted. The findings from both theoretical and experimental workspace are then compared and discussed. Finally, conclusions are drawn and future work is presented.

## 2. THE MICRO-MOTION STAGE DESIGN

The micro-motion system presented in this paper is also known as 3RRR compliant mechanism. It is a monolithic compliant mechanism utilising flexure hinges. The stage is actuated by three PZT stack actuators as shown in Figure 1 and is designed based on the 3RRR mechanism structure as depicted in Figure 2.

---

<sup>\*</sup> Corresponding author: [tien-fu.lu@adelaide.edu.au](mailto:tien-fu.lu@adelaide.edu.au); phone +61 8 83033556; fax +61 883034367; School of Mechanical Engineering, the University of Adelaide, North Terrace, Adelaide, SA 5005, Australia; <http://www.mecheng.adelaide.edu.au/robotics/index.html>

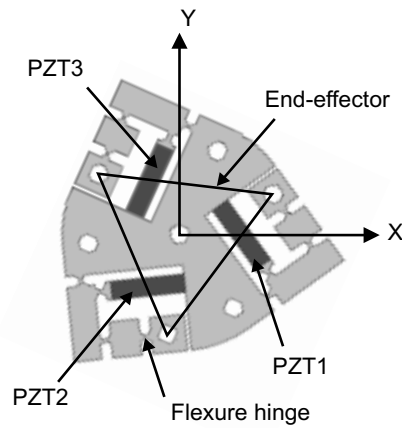
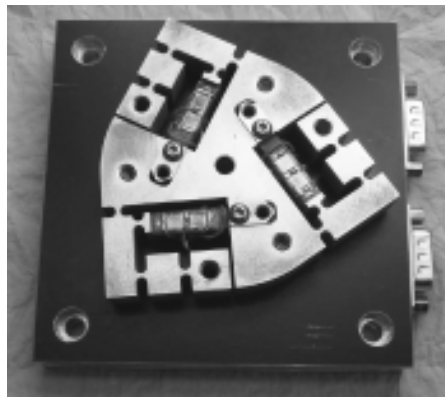


Figure 1: 3RRR compliant micromanipulation device

### 3. PSEUDO RIGID BODY MODEL

The pseudo-rigid-body model approach and loop-closure theory were adopted to derive the linear kinematics of the presented compliant micro-motion stage<sup>8</sup>. The PRBM is used to model the deflections of the flexible members using conventional rigid-link mechanism theory. The PRBM assumes that the flexure hinges in the structure act like revolute joints with torsional springs attached to them. The other parts of the structure are assumed to be rigid. The PRBM of the presented 3RRR compliant mechanism is illustrated in Figure 2. Loop-closure theory incorporates the complex number method to model a mechanism. For each closed-loop in the mechanism, a loop equation is generated<sup>9</sup>. This equation can be expressed in terms of its real and imaginary parts, resulting in two equations per loop. Unknowns can be found by solving these equations simultaneously. The modeling result of this approach has been proved to be as good as the models derived by other researchers<sup>8</sup>.

A Jacobian matrix is normally used to relate the velocity of an end-effector to the velocity of actuators. However, for the case of compliant micro-motion stages, the Jacobian matrix can be defined as a matrix to relate  $(\Delta l_1, \Delta l_2, \Delta l_3)$  with  $(\Delta x, \Delta y, \Delta \theta)$ <sup>10</sup>. The displacements of the PZT actuators are small compared to the link lengths and hence the motion range of the 3RRR mechanism is also small. Therefore, the micromanipulation stage is almost configurationally invariant and its Jacobian matrix is assumed to be constant:

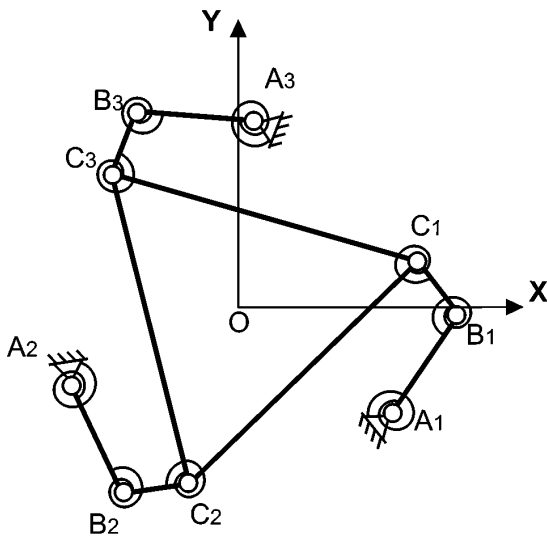


Figure 2: 3RRR compliant mechanism

The end-effector platform is attached to the ends of the three linkages as illustrated by a triangle in Figure 1. The end-effector translates along x, y-axis and rotates about the z-axis.

Rather than stacking three 1-DOF stages together to obtain 3-DOF movement that accumulates errors, this parallel design does not accumulate errors (Abbe errors). This type of parallel structure is also more rigid and lighter weight than a serial manipulator using stacked stages. The disadvantage of a parallel design is that the kinematics and dynamics can be complicated leading to complex models and controller design. However, the presented manipulator has been proved to be uncoupled<sup>7</sup>, which simplifies the model and control design.

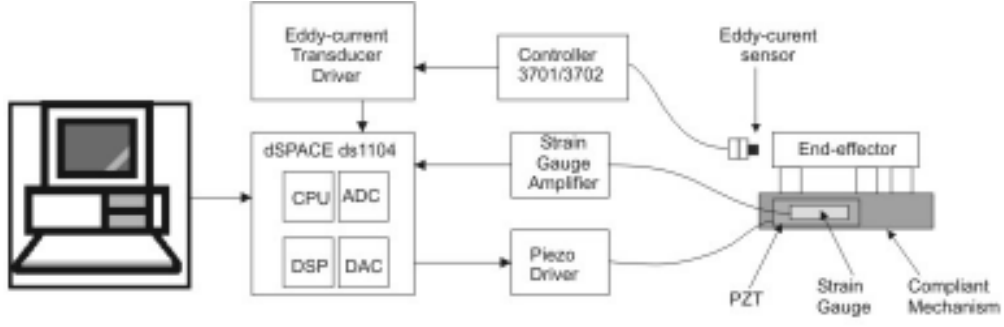


Figure 3: Schematic of the experimental set-up

$$\begin{bmatrix} \Delta x \\ \Delta y \\ \Delta \gamma \end{bmatrix} = J \begin{bmatrix} \Delta l_1 \\ \Delta l_2 \\ \Delta l_3 \end{bmatrix} \text{ where} \quad (1)$$

$$J_{\text{exp}} = \begin{bmatrix} 0.668 & -1.298 & 0.734 \\ -1.183 & -0.0017 & 1.361 \\ -25.433 & -24.975 & -26.073 \end{bmatrix} \quad (2)$$

$$J_{\text{theoretical}} = \begin{bmatrix} 1.905 & -3.220 & 1.315 \\ -2.618 & -0.341 & 2.959 \\ -59.960 & -59.960 & -59.960 \end{bmatrix}$$

With such a simple constant matrix, the calculations for forward and inverse kinematics of the compliant micro-motion stage are more efficient than using any other mathematical models.

#### 4. EXPERIMENTAL SET-UP

The experimental set-up of the micro-motion system consists of 3 Tokin AE0505D16 PZT stack actuators assembled into a flexure hinge, compliant mechanism, as shown in Figure 1. Each unloaded actuator has a maximum displacement of approximately 15  $\mu\text{m}$ . These PZTs are each driven by a Physik Instrumente (PI) PZT amplifier, which provides a bi-polar voltage ranging from  $-20\text{V}$  to  $120\text{V}$ . The amplifiers have a maximum output power of 30W. Measurement Group EA-06-125TG-350 strain gauges are mounted to the PZTs to determine their displacement. All the strain gauges are connected to a strain gauge conditioner. The end-effector location is measured using three Micro-Epsilon eddyNCDT 3700 eddy-current transducers. The PZT amplifiers, strain gauge conditioning circuitry and eddy-current transducers are connected to a dSPACE DS1104 DSP controller board via inbuilt DAC's and ADC's. A schematic of the experimental set-up is shown in Figure 3.

For comparison purpose, an experimental constant Jacobian is obtained out of the experimental data relating the extensions of PZTs with the end-effector movement. The experimentally derived Jacobian matrix is given below.

#### 5. WORKSPACE ANALYSIS where (1)

The theoretical workspace is obtained by using the theoretical Jacobian, Equation (1). All possible combinations of elongation produced by each of the three PZT actuators,  $(\Delta l_1, \Delta l_2, \Delta l_3)$ , from 0 to 10  $\mu\text{m}$  with 0.5 $\mu\text{m}$  increment, are input to the Jacobian to generate corresponding end-effector displacements  $(\Delta x, \Delta y, \Delta \gamma)$  that fill the workspace. The workspace is shown in Figure 4 with the rotation of the end-effector,  $\Delta \gamma$  given on the z-axis. Figure 4a is a top view of the workspace, looking at the x-y plane, and shows the reachable workspace area. Figure 4b and 4c show the front and side views of the workspace respectively, where the vertical axis is the rotation,  $\Delta \gamma$ . Three slices have been taken through the workspace. These show the workspace area in the x-y plane at different angles of rotation, as shown in Figure 5.

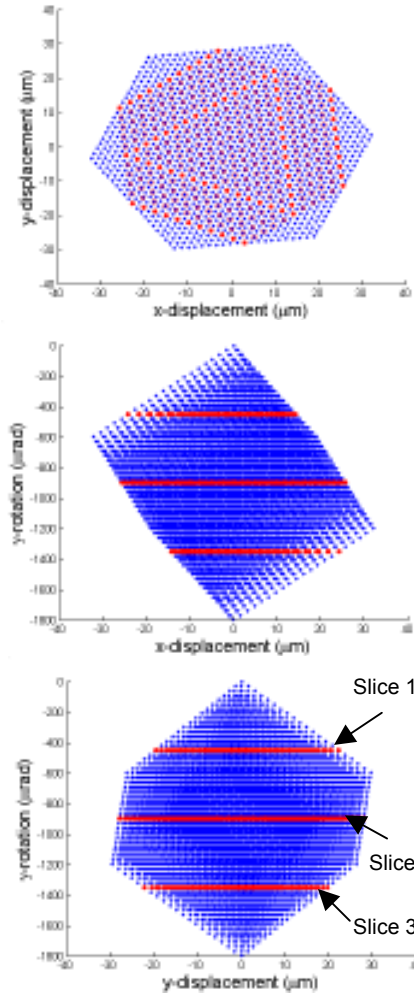


Figure 4 : The theoretical workspace of the 3RRR micro-motion system. a.) the top, x-y plane, view of the workspace, b.) and c.) the front and side views of the workspace, the rotation is given along the vertical-axis

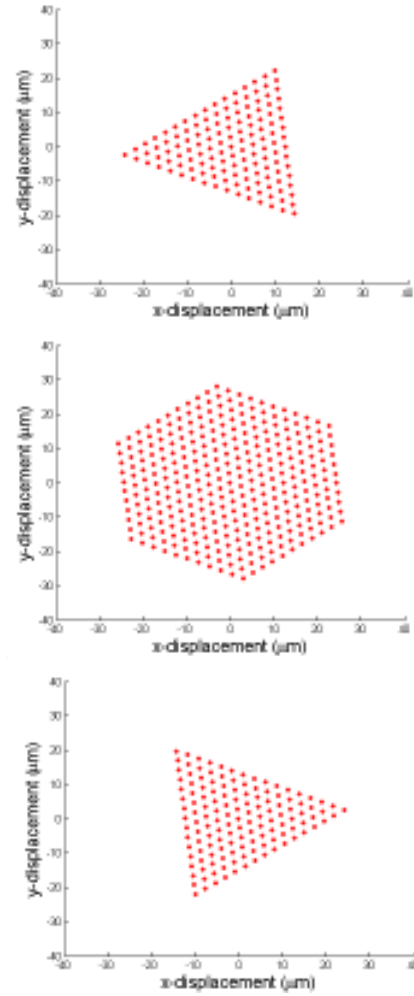


Figure 5: Slices taken through the workspace at different angles of rotation, a.) Slice 1, rotation is  $-450\mu\text{rad}$ , b.) Slice 2, rotation is  $-900\mu\text{rad}$ , c.) Slice 3, rotation is  $-1350\mu\text{rad}$

From Figure 5 it can be noted that the largest workspace area in which the end-effector has a constant angle of rotation is when the angle of rotation is  $-900\mu\text{rad}$ . The point at the centre of this slice,  $\Delta x = \Delta y = 0$ ,  $\Delta \gamma = -900\mu\text{rad}$ , corresponds to input displacements of  $\Delta l_1 = \Delta l_2 = \Delta l_3 = 5\mu\text{m}$ . This is the centre of the workspace.

The experimental workspace is obtained by using the experimentally determined Jacobian, Equation (2), in the same manner as to determine the theoretical workspace. The workspace is shown in Figure 6. The views given are the same as the theoretical workspace figures.

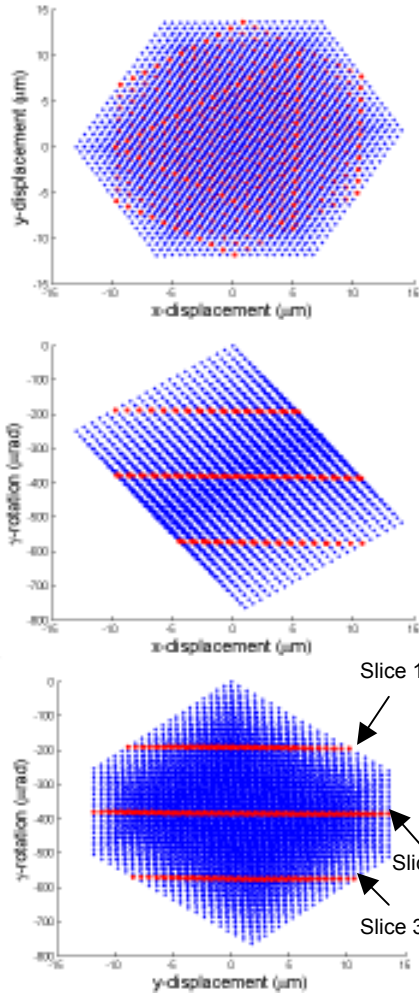


Figure 6: The experimental workspace of the 3RRR micro-motion system. a.) the top, x-y plane, view of the workspace, b.) and c.) the front and side views of the workspace, the rotation is given along the vertical-axis

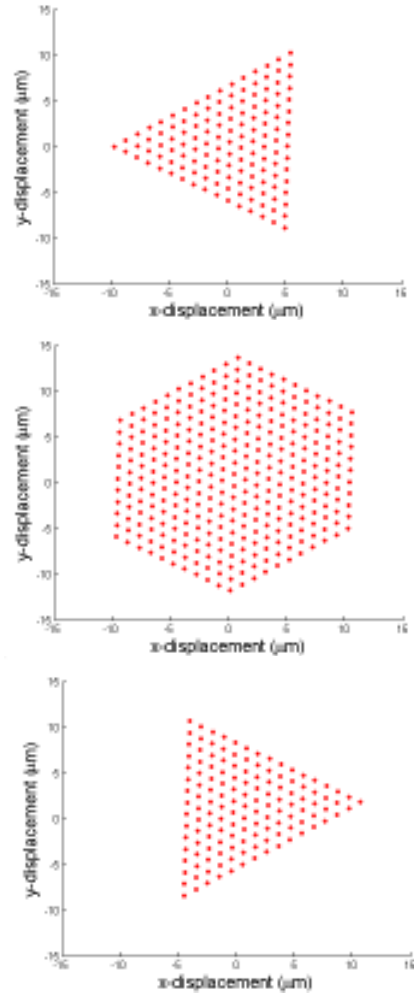


Figure 7: Slices taken through the workspace at different angles of rotation, a.) Slice 1, rotation is  $-192\mu\text{rad}$ , b.) Slice 2, rotation is  $-382\mu\text{rad}$ , c.) Slice 3, rotation is  $-572\mu\text{rad}$

From Figure 7 it can be noted that the largest workspace area in which the end-effector has a constant angle of rotation is when the angle of rotation is  $-382\mu\text{rad}$ . The point at the centre of this slice,  $\Delta x = \Delta y = 0$ ,  $\Delta \gamma = -382\mu\text{rad}$ , corresponds to input displacements of  $\Delta l_1 = \Delta l_2 = \Delta l_3 = 5\mu\text{m}$ . This is the centre of the workspace.

## 5. COMPARISON OF RESULTS

From Figures 4 to 7 it can be observed that the theoretical workspace is significantly larger than the experimental workspace. To make this comparison clearer the theoretical and experimental workspace areas through the centre of the workspace are shown together in Figure 8. The height and width of the experimental workspace are 46% and 40% of the theoretical workspace respectively. It will also be noted that the workspace areas are a similar shape though rotated relative to each other.

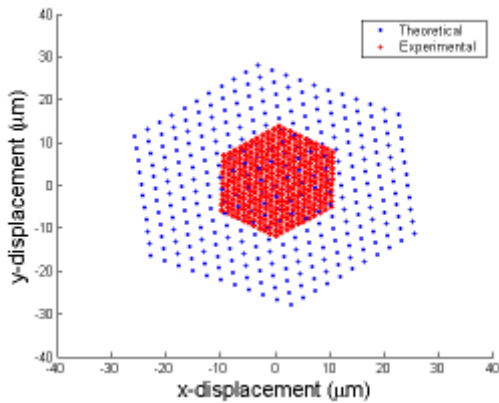


Figure 1: comparison of theoretical and experimental workspace areas, through the centre of the workspace.

The very significant difference in workspace area prompted further experimental investigation. During this investigation the displacement of the PZT pre-load mechanism was studied. This mechanism can be seen in Figure 1 as a block at the base of each PZT. Theoretically this block should not displace at all, but it was considered highly likely that in the real system it might displace a small amount. It was found that for a PZT displacement of  $10\mu\text{m}$  the displacement of the preload block was just over  $3\mu\text{m}$ . The block acted as a spring and returned to its original position when the PZT displacement returned to zero. This suggests that were the block to be fixed solidly the experimental workspace would be over 30% larger than given in these current results. The theoretical and experimental results would then be far closer.

## 6. CONCLUSIONS AND FUTURE WORK

This paper presented the workspace of a 3 degree-of-freedom compliant micro-motion stage with flexure hinges. This micro-motion stage has parallel structure and can be implemented for applications requiring motions in micrometres or even nanometres. Possible applications include micro-system assembly, biological cell manipulation and microsurgery. In this paper both the theoretical and experimentally determined workspaces were presented and compared. The two workspaces were shown to have similar shapes although the experimental workspace area is significantly smaller than predicted by the theoretical workspace. Further investigation revealed that this discrepancy is partly due to undesired movement of the PZT preload block. In future work the preload mechanism will be redesigned so that it is solidly fixed and does not flex under load. The experimental Jacobian and workspace can then be determined once more and compared to the theoretical workspace. The accuracy of the theoretical kinematic model will then be assessed and if necessary model improvements will be made. If the kinematic model can be proven to be relatively accurate then it will be used for optimal

design of the compliant mechanism. This optimal design will not only consider kinematics but also the coupling of the mechanism and dynamic behaviour. The kinematics and workspace requirements are the fundamental requirements of the manipulator to be achieved before considering aspects such as operating frequency and trajectory tracking capabilities.

## REFERENCES

- <sup>1</sup> F. Scire and C. Teague, "Piezodriven 50- $\mu\text{m}$  range stage with subnanometer resolution," *Rev. Sci. Instrum.*, 49(12), 1735-1741, 1978.
- <sup>2</sup> I. Her and J. C. Chang, "A linear scheme for the displacement analysis of micropositioning stages with flexure hinges," *Journal of Mechanical Design, Trans. ASME*, 116, 770-776, 1994.
- <sup>3</sup> P. Gao, S. Swei and Z. Yuan, "A new piezodriven precision micropositioning stage utilizing flexure hinges," *Nanotechnology*, 10, 394-398, 1999.
- <sup>4</sup> Pasi Kallio, Quan Zhou, Mikael Lind, Keikki N. Koivo, "Position Control of a 3 DOF Piezohydraulic Parallel Micromanipulator," IEEE/RSJ International Conference on Intelligent Robotic Systems, October 13-17, 1998, Victoria, B.C., Canada,
- <sup>5</sup> O. Ma and J. Angeles, "Direct kinematic and dynamics of a planar three-dof parallel manipulator," *Advances in Design Automation*, 2, 313-320, 1993.
- <sup>6</sup> A. Codourey, "Dynamic modeling of parallel robots for computed-torque control implementation," *The International Journal of Robotics Research*, 17(12), 1325-1336, 1998.
- <sup>7</sup> Daniel Handley, Wei Zhao, W. J. Zhang, Q. Li and Tien-Fu Lu, "An Experimental Observation of Uncoupling of Multi-DOF PZT Actuators in a Compliant Mechanism," 7<sup>th</sup> International Conference on Control, Automation, Robotics and Vision (ICARCV'02), Dec 02, Singapore
- <sup>8</sup> Yong, Y.K.; Lu, Tien-Fu; Handley, D., "Loop Closure Theory in Deriving a Linear and Simple Kinematic Model for a 3 DOF Parallel Micro-motion System," the SPIE's International Symposium on Microelectronics, MEMS, and Nanotechnology, 10-12 December 2003, Perth, Australia
- <sup>9</sup> L. L. Howell and A. Midha, "A Loop-Closure Theory for the Analysis and Synthesis of Compliant Mechanisms," *Journal of Mechanical Design*, 118, 121-125, 1996.
- <sup>10</sup> W. J. Zhang, J. Zou, G. Watson, W. Zhao, G. Zong and S. Bi, "Constant-Jacobian Method for Kinematics of a 3-DOF Planar Micro-Motion Stage," *Journal of Robotic Systems*, 19(2), 63-79, 2002.